ARMY RESEARCH LABORATORY

Model of High-Energy-Density Battery Based on SiC Schottky Diodes

by Yves Ngu, Marc Litz, and Bruce Geil

ARL-TR-3981 **Ocotber 2006**

NOTICES

Disclaimers

The findings in this report are not to be construed as an official Department of the Army position unless so designated by other authorized documents.

Citation of manufacturer's or trade names does not constitute an official endorsement or approval of the use thereof.

Destroy this report when it is no longer needed. Do not return it to the originator.

Army Research Laboratory
Adelphi, MD 20783-1197

ARL-TR-3981 **October 2006**

Model of High-Energy-Density Battery Based on SiC Schottky Diodes

Yves Ngu, Marc Litz, and Bruce Geil
Sensors and Electron Devices Directorate, ARL

REPORT DOCUMENTATION PAGE

Form Approved
OMB No. 0704-0188

1. REPORT DATE *(DD-MM-YYYY)*	2. REPORT TYPE	3. DATES COVERED (From - To)
October 2006	Progress	January to July 2006

4. TITLE AND SUBTITLE
Model of High-Energy-Density Battery Based on SiC Schottky Diodes

5a. CONTRACT NUMBER

5b. GRANT NUMBER

5c. PROGRAM ELEMENT NUMBER

6. AUTHOR(S)
Yves Ngu, Marc Litz, and Bruce Geil

5d. PROJECT NUMBER

5e. TASK NUMBER

5f. WORK UNIT NUMBER

7. PERFORMING ORGANIZATION NAME(S) AND ADDRESS(ES)
U.S. Army Research Laboratory
ATTN: AMSRD-ARL-SE-DE
2800 Powder Mill Road
Adelphi, MD 20783-1197

8. PERFORMING ORGANIZATION REPORT NUMBER
ARL-TR-3981

9. SPONSORING/MONITORING AGENCY NAME(S) AND ADDRESS(ES)
U.S. Army Research Laboratory
2800 Powder Mill Road
Adelphi, MD 20783-1197

10. SPONSOR/MONITOR'S ACRONYM(S)

11. SPONSOR/MONITOR'S REPORT NUMBER(S)

12. DISTRIBUTION/AVAILABILITY STATEMENT
Approved for public release; distribution unlimited.

13. SUPPLEMENTARY NOTES

14. ABSTRACT
Silicon carbide (SiC) diodes are being investigated as direct energy converters (DECs) for use in small, long-lived nuclear power sources for unattended sensors. Voltage and current measurements on Schottky diodes fabricated from both Si and SiC result in typical efficiencies of 5 to 15%. A drift-diffusion model has been developed to predict the output and to help us better understand the radiation-induced current that results. This report describes the initial conditions, the drift-diffusion algorithm, and the material parameters used in the model. The results of the model compare well to experimental data.

15. SUBJECT TERMS
Silicon carbide, schottky model, DEC

16. SECURITY CLASSIFICATION OF:			17. LIMITATION OF ABSTRACT	18. NUMBER OF PAGES	19a. NAME OF RESPONSIBLE PERSON
a. REPORT	b. ABSTRACT	c. THIS PAGE	SAR	20	Yves Ngu
Unclassified	Unclassified	Unclassified			19b. TELEPHONE NUMBER (*Include area code*) 301-394-5541

Standard Form 298 (Rev. 8/98)
Prescribed by ANSI Std. Z39.18

Contents

List of Figures

List of Tables

1. Background

Nuclear batteries can have a small but significant impact as a power source for long-lived sensors (*1-3*). Consider embedded sensors for bridges and foundations of large buildings. These sensors can provide information about the structural integrity (*4-6*). Unattended sensors for temperature measurement in the oceans would need no maintenance during an increased operational lifetime. Unique opportunities are waiting for sensors that benefit from "keep-alive" power lasting decades.

Chemical power sources can store the total energy required, but electrical leakage and deterioration of the batteries keep them from delivering the power over a decade. Nuclear batteries offer a unique power source to fill the niche. Even though the energy-density of nuclear isotopes is six orders of magnitude greater than that possible in chemical bonds, the stigma associated with nuclear materials will require careful design and thoughtful application. Sensors embedded in structures, which provide information useful to monitor structural integrity (i.e., bridges, helicopter blades), may be just the application to overcome these difficulties.

Semiconductor based radioisotope power converters use the energy generated by the decay of radioisotopes to create a power source. A battery of this type is composed of three main parts: 1) a radioisotope source of high energy density, 2) an energy converter (diode) that changes the radiation output of the radioisotope energy source into some form of usable electrical energy, and 3) a load that can consume or store the electrical energy. A simple nuclear battery design consists of alternating layers of isotope, sandwiched in between layers of silicon carbide (SiC) diodes. A sample battery in AA format is currently being constructed. The isotope consists of 11 each, 50-µm-thick, 2-mm-diameter foils of nickel (63Ni). The 63Ni is surrounded by layers of SiC diodes. The diodes are 5-mm-square, 400-µm-thick devices.

The goal of this report is to establish a model for the direct energy converter (DEC), as well as to characterize the impact of the load on the output power generated. The model will enable us to predict device efficiency and improve the efficiency in future design iterations. One way to improve battery efficiency is to match the penetration of beta (or gamma) decaying from the isotope, to the range of penetration (stopping power) of the DECs. The DEC undergoing consideration is a SiC based Schottky diode, as seen in figure 1.

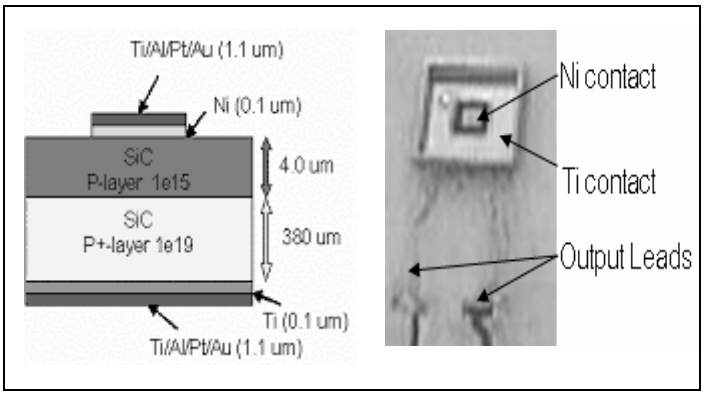

Figure 1. SiC Schottky diode.

Section 1 identifies the motivation for our efforts and discusses some of the applications that will benefit from the investigations. Section 2 discusses the overall approach taken in the model. Section 3 describes details of the model and values of material parameters applied. Section 4 details the significant results, and section 5 provides conclusions and impacts of these results on the larger goal of developing efficient nuclear batteries for long-lived sensors.

2. Approach

The energetic particles emitted during the decay of the radioisotopes create a multitude of electron-hole pairs within a semiconductor. The distribution of generated carriers is modeled via a Monte Carlo radiation transport code (MCNPX) and has been examined previously (*7*). Once the carriers are generated, we have positive charges flowing into the semiconductor, leading to a generated current Ig which is equivalent to a short circuit current (Isc). The displaced carriers effectively forward biases the p-layer, as seen in figure 2(a). The forward bias junction yields a current (Id) through the junction, opposing the generated current. In the presence of very small load (short), Isc = Id while the output voltage with very high load (open) is Voc, the open circuit voltage. When a load is connected to the diode's output terminals as in figure 2(b), the current attributable to the forward bias junction is split between the current into the load (Iout) and Id so that Ig = Id + Iout.

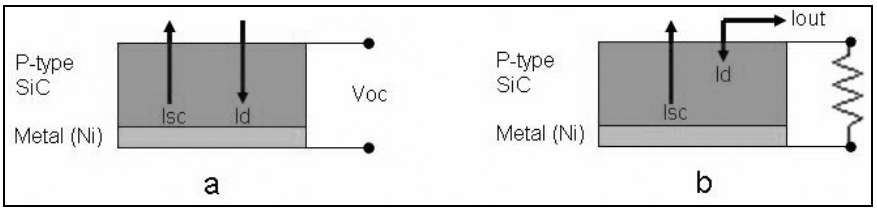

Figure 2. Current flow under a) open circuit and b) load condition.

The objective is to estimate how the diode's structure and the connected load affect the output voltage of the battery. The structure of the diode defines the generated current (Ig). Furthermore, the "leakage current" (Id, forward current) in the diode determines the amount of lost current. Omitting the radioisotope layer (which would be in direct contact with the Schottky contact of the diode—Ni/Ti/Al/Pt/Au metal layer), the diode and the load are modeled by the equivalent circuit displayed in figure 3.

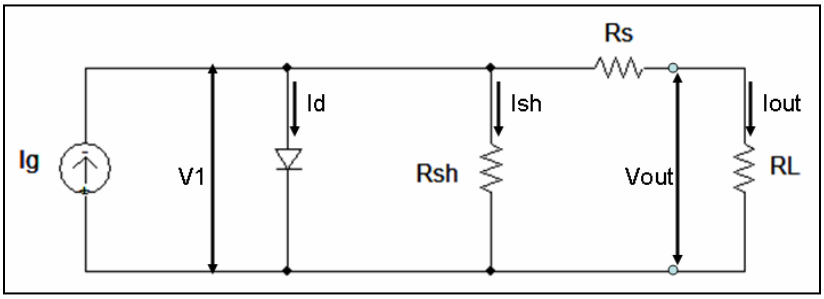

Figure 3. Equivalent circuit of diode and load.

The values of components of figure 3 are derived from material properties of the semiconductor. The devices presently being evaluated are SiC Schottky diodes using nickel as metal contact. Most of the material properties of SiC were obtained from literature (*8*) and are tabulated in table 1. In figure 3, RL represents the load resistance, and the components for which values and expressions need to be determined are Rsh, Rs, Ig, and Id in which

- Rsh is the shunt resistance that arises from leakage of current around the cell, via the edges of the device. It is estimated as the resistance present across the diode at 10 mV forward bias.
- Rs is the series resistance attributable to contacts and internal resistance of the diode.
- Ig is the generated electron current (dependent on carriers within the depletion region as well as those outside, with collection efficiency higher when closer to depletion region).
- Id is the current flowing in the diode attributable to the forward biased junction ("leakage current").

Table 1. Material properties of SiC.

Parameter	Symbol	Value (unit)
Intrinsic Conc.*	n_i	1.6E-6 (cm^{-3})
Electron Affinity*	X	3.5 (eV)
Band Gap*	E_g	3.23 (eV)
Dielectric Constant*	K_s	9.66 (cm^2/V-s)
Recombination Coef.*	Rc	1.5E-12
Hole Mobility*	u_p	120 (cm^2/V-S)
Electron Mobility*	u_e	900 (cm^2/V-S)
Diffusion Length*	L	1.5E-4 (cm)
Doping Level	N_a	1E15 (cm^{-3})
Build in Voltage**	V_{bi}	0.86 (eV)
Schottky Barrier**	V_{bar}	0.95 (eV)
Device Area	Area	0.25 (cm^2)
Ni Work Function	work_Ni	5.15 (eV)

*Extracted from (*2*)
**Assumes Fermi level is pinned (*4*)

3. Circuit Model

The various components values are determined by basic semiconductor equations that use the doping level and size described in figure 1, with the top SiC layer referred to as active layer and the bottom layer as the substrate. The concentration of carriers generated within the depletion region is identified as *Conc(in)*, whereas the concentration of carriers generated outside the depletion region is identified as *Conc(out).* The model for the shunt resistance, *Rsh*, is given in equation 1. It is derived from the diode current expression for a diode at 10 mV forward bias. Equation 2 is the model of series resistance, *Rs*, where the contact resistance was neglected. Equation 3 gives an expression for the generated current, *Ig*. This current is attributable to electron carriers. It is assumed that electrons located within the depletion region, which have acceptable energy values (discussed in the next section), will have a collection efficiency of a 100% (fully contribute to drift current). Alternately, carriers generated outside the depletion region will have an exponential collection efficiency, where *X* is the distance between the carrier and the edge of the depletion region, and *L* is the diffusion length. Equation 4 refers to diode "leakage current", which is controlled by the output current and load resistance.

$$Rsh = \frac{10e3}{\text{Area} * \text{Jsat} * (\exp\frac{\text{10e - 3}}{\text{k} * \text{T}} - 1)} \tag{1}$$

$$Rs = \frac{1}{\text{q} * \text{up} * \text{Area}} * \left(\frac{Wactive}{Na} + \frac{Wsubstrate}{Nsub} \right) \tag{2}$$

$$Ig = \frac{q^2 * up * Na * W * Area}{2 * \mathrm{Ks} * \mathrm{eo}} * \left(Conc(in) + Conc(out) * \exp\frac{-X}{L} \right) \tag{3}$$

$$Id = Isat * \exp\frac{Iout * (Rs + RL)}{k * T} - 1 \tag{4}$$

In the equations above, *Ks* is the coefficient describing the relative dielectric constant *eo*, *up* is electron mobility, *Wactive* is the thickness of upper SiC layer, and *W* is the thickness of the depletion region.

All these equations were modeled with MATLAB[1]. Equation 5 allows us to solve for the internal diode voltage, *V1*. *V1* is then used to determine the output voltage and current with equations 6 and 7, respectively. Finally, *Vout* versus *RL*, *Iout* versus *RL*, and *Vout* versus *Iout* are all plotted as our results.

$$Ig = Id + \frac{V1}{\mathrm{Rsh}} + \frac{V1}{RL + Rs} \tag{5}$$

$$Vout = RL * \frac{V1}{RL + Rs} \tag{6}$$

$$Iout = \frac{V1}{RL + Rs} \tag{7}$$

4. Results

As mentioned in the previous section, carriers contributing to the generated current require an acceptable energy level. The idea of acceptable energy level results from the fact that carriers generated by beta sources have a large range of kinetic energy. Once these carriers are introduced in our device, not all of them can contribute to current. Most of the contribution is supported by the lower energy (<50 keV) electrons (*7*). Generally, in such a system, many physical phenomena such as secondary electron production, hole-electron pair generation, cathod-luminescence, x-ray generation, and other processes contribute to energy losses (*9*).

The lower energy electrons contribute more to electrical power output because their energy is more easily collected by the diode. From the electron energy spectrum (*7*), we can estimate that about 5 of every 1000 generated carriers have energy comparable to that exerted by the device's internal electric field. Consequently, to a first order approximation, the concentration of carriers obtained from MCNPX simulation can be scaled by $0.2e^{-3}$ to represent the carriers relevant to current generation.

[1]MATLAB is a registered trademark of the MathWorks.

The results of the numerical simulation, based on the equations described in section 3, produce reasonable values for the unknown parameters of the current into the load, *Iout*, and voltage across the load, *Vout*. The current Iout and the voltage Vout are measured values in the experimental verification of this model. These values are measured as a function of RL, the load resistance. The load resistance is varied from 1 Ω to 1 MΩ. The numerical results for these simulations are shown in figures 4, 5, and 6.

Figure 4 is a plot of Vout versus RL, figure 5 is a plot of Iout versus RL, and figure 6 is a plot of Iout versus Vout. In figure 4, the curve deviates from the straight line curve that would be expected from a resistive circuit. This behavior is attributable to the increased "leakage current" (Id) via the diode (see figure 3) as Vout increases. With increased load, Vout increases as well as Id; thus, the slope of Vout versus RL decreases and curvature can be observed. This curvature is also present in figure 5 where it can be seen that less and less of the generated current (Ig) flows through RL. Figure 6 is in a sense a combination of figures 4 and 5. The shape of this curve mimics the typical response of photovoltaic cell. The output current is maximum (Iout = Isc = 95 nA) when the Vout = 0 (output shorted yielding short circuit current). The maximum output (Vout = Voc = 0.15V) occurs at near zero output current (the load is extremely large yielding open circuit voltage).

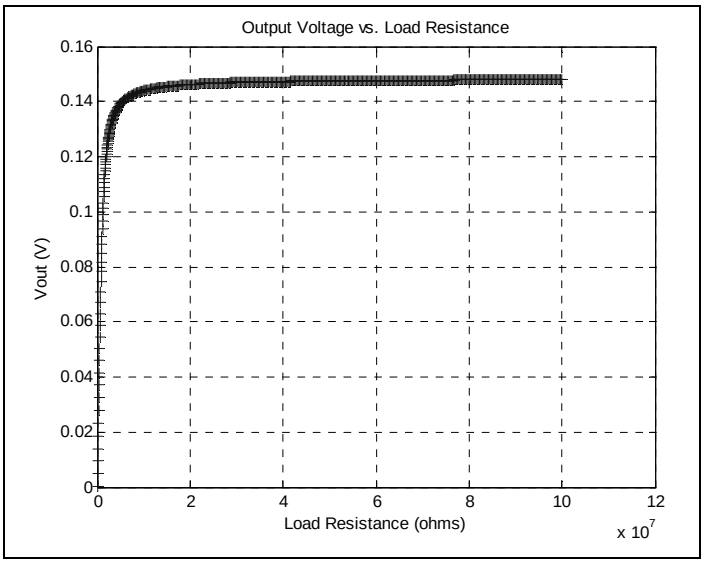

Figure 4. Vout versus load resistance simulated results.

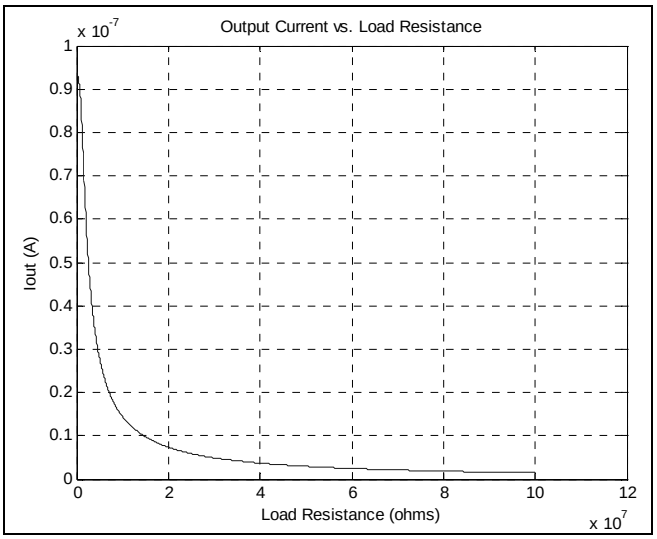

Figure 5. Iout versus load resistance simulated results.

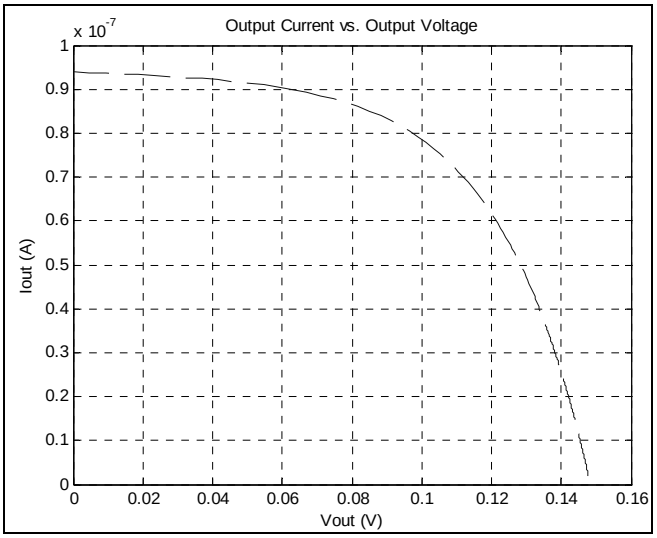

Figure 6. Iout versus Vout simulated results. (The Voc is 150 mV and the Isc is 950 nA.)

Throughout this analysis, the generated current was described by equation 3. In this equation, the concentration distribution is obtained from MCNPX and described in discrete form. Furthermore, equation 3 is based on the electric field inside the depletion region (described by equation 8). The "½" in the equation is used to obtain an average field within the depletion region. This average field multiplied by the concentration of generated charge, their mobility, and the device area (as described in equation 3) should yield the overall generated current. However, it was noted that equation 8 is a poor description of average electric field, assuming that the presence of an average field within the depletion region is somewhat incorrect.

$$Efield = \frac{q * Na * W}{2 * \mathrm{Ks} * \mathrm{eo}} \tag{8}$$

In a photodiode with a given photgeneration rate (Gen) and assuming this rate to be uniform throughout the diode, the generated current should be described by equation 9. In this equation, all the minority carriers (electrons) created within the depletion region (W) and one diffusion length (L) await from the junction are swept by an electric field to the opposite side of the junction derby yielding a current. This approach also holds in the case of carriers generated by radioisotope particles except that the generation rate is no longer uniform. However, the generated charge distribution obtained from MCNPX was curve fitted to yield generation function (Gen(x)) that is position dependent (see equation 10). In equation 10, "*events*" describes the particle emission rate of the radioisotope (number of events per second). The generated current can be represented by equation 11, which is a modified version of equation 9 for non-uniform distribution rate and the derivative is taken from 0 (schottky junction) to W+L (distance of the farthest electron that can be collected).

$$Ig = q * Area * (W + L) * Gen \tag{9}$$

$$Gen(x) = events * 2.9e4 * \exp^{-0.014 * x} \tag{10}$$

$$Ig = q * Area * \int_{0}^{W+L} Gen(x)dx \tag{11}$$

The generated current obtained with equation 11 was introduced in our original equivalent circuit and the output curves obtained are plotted in figures 7, 8, and 9.

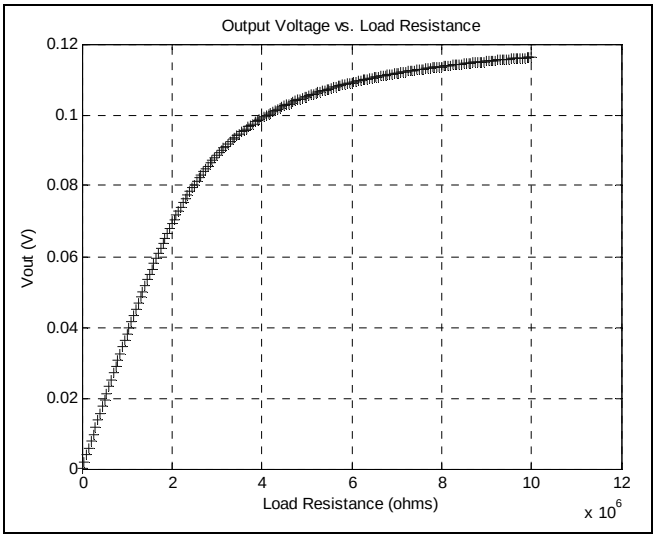

Figure 7. Vout versus load resistance simulated results with Gen(x).

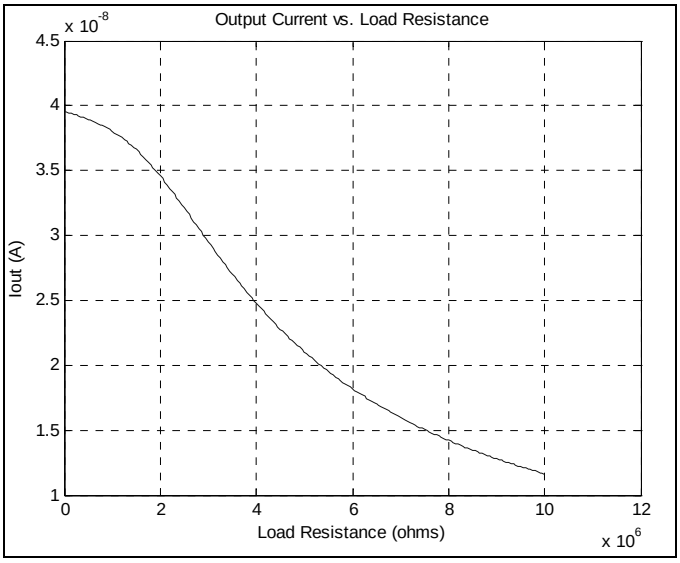

Figure 8. Iout versus load resistance simulated results with Gen(x).

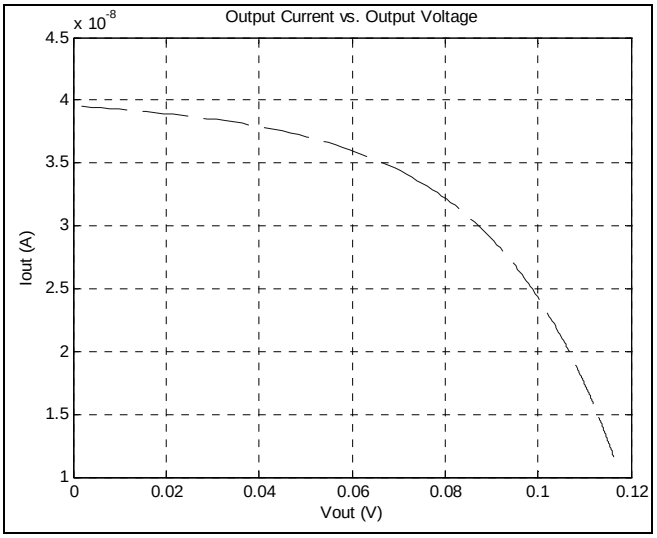

Figure 9. Iout versus Vout simulated results. (The Voc is 120 mV and the Isc is 40 nA.)

5. Conclusions

The model showed some dependency on load resistance value. To further understand what might be happening, an analysis of the effects of Schottky contact metal (work function) and generated carrier concentration was undertaken.

It is noted that an increase in generated carrier concentration led to “similar increase in generated carriers (one order magnitude increase in generated carrier led to approximately one order of magnitude increase in current). Also, as the carrier concentration was increased, the I-V curve of the device displayed an increase bending (knee), as would be expected in the case of a photovoltaic. As the carrier concentration is decreased, the bending of the I-V curve is lost. This is probably because at low current, the output voltage is low, making the diode component (Id) of the model negligible, rendering the behavior of the circuit similar to that of a resistive circuit. In this way, the model behavior resembles that of a simple resistive circuit.

Simulations were also run to determine the effect of the metal used for the Schottky contact. The parameter changed to indicate that change in metal was the metal work function value. This is the minimum energy that must be given to an electron to liberate it from the surface of a particular metal. Changes of the metal (work function) used for the Schottky contact indicated that as a metal with small work function is used, the generated current is increased via greater built-in voltage, barrier voltage, depletion region, and maximum electric field in the depletion region.

The model established in this document has two distinct modes of operation. On the one hand, all the semiconductor voltages (built-in and barrier) are obtained from basic semiconductor equation. On the other hand, the assumption was made that the electronic behavior of our SiC devices displays a Fermi level pinning effect. According to (*4*), the lattice imperfection existing near the surface of the SiC (defect level with activation energy=0.96eV) leads to the pinning of the Fermi level in p-type SiC. This behavior yields a fixed barrier voltage of about 0.95eV with nickel, independent of the SiC doping concentration. This pinning also makes negligible any effects attributed to the Schottky metal work function since the built-in voltage and barrier voltage are about constant.

When we compared the simulation made with and without Fermi level pinning, it was observed that the absence of pinning yielded currents one order of magnitude greater. Not only was the current level greater, but so was the open circuit voltage. The values obtained were much more removed from the experimental results (numerically and curve shape) than was the case when Fermi level pinning was assumed. In both cases, it was noted that generated carrier concentration was directly linked to the value of generated current (increasing charge concentration increases generated current) although the current levels assuming Fermi level pinning were much lower. The lower current is because the pinned Fermi level generates a lower built-in voltage, barrier voltage, depletion region, and electric field inside the depletion region.

It was noticed that the electric field within our Schottky diode could not be assumed as constant, as described in equation 8. Drawing some parallelism between our DEC and typical photodiode, the generated current can be determined independently of the internal field. The assumption in this case is that the depletion region volume times the generation rate would yield generated

current (charge/sec). This current is derived by equation 11. This approach gives way to a generated current that is closer to experimental results compared to the other technique. However, the trends described in the previous paragraphs still hold.

The model has been established for our battery system. The behavior of the battery can be predicted, given the load. However, we still need to determine accurately what values to use for our collection efficiency and to more precisely describe the carrier generation rate. This will enable output currents to be in the same range as our experimental values.

6. References

1. Blanchard, James P. Stretching the Boundaries of Nuclear Technology. *The Bridge* 32.4, 2002, 29-34.
2. Ahearne, John F. The Future of Nuclear Energy. Editorial. *The Bridge* 31.3, 2001, 3.
3. Bugliarello, George. Our Energy Future. Editorial. *The Bridge* 32.2, 3-4.
4. Lal, Amit; Blanchard, James. The Daintiest Dynamos. *IEEE Spectrum* **Sept. 2004**, 36-41.
5. Lal, A.; Blanchard, James. By Harvesting Energy From Radioactive Specks, Nuclear Micrbatteries Could Power Tomorrow's Microelectromechanical Marvels-And May Be Your Cellphone Too. *IEEE Spectrum* **September 2004**, 36-41.
6. Litz, M.; et al. On-Demand High Energy Density Materials. *Amer. Inst. of Aero. and Astro*.
7. Litz, M.; Blaine, K. *Isotope Generated Electron Density in Silicon Carbide Direct Energy Converters*; ARL-TR-3964; U.S. Army Research Laboratory: Adelphi, MD, August 2006
8. Levinstein, M.; et al. *Properties of Advanced Semiconductor Materials: GaN, AlN, InN, BN, SiC, SiGe*. John Wiley & Sons (2001).
9. Everhart, T. E.; Hoff, P. H. Determination of Kilovolt Electron Energy Dissipation vs Penetration Distance in Solid Material. *Journal Appl. Phys.* **December 1971**, *42* (13).

Distribution List

ADMNSTR
DEFNS TECHL INFO CTR
ATTN DTIC-OCP (ELECTRONIC COPY)
8725 JOHN J KINGMAN RD STE 0944
FT BELVOIR VA 22060-6218

DARPA
ATTN IXO S WELBY
3701 N FAIRFAX DR
ARLINGTON VA 22203-1714

OFC OF THE SECY OF DEFNS
ATTN ODDRE (R&AT)
THE PENTAGON
WASHINGTON DC 20301-3080

US ARMY RSRCH DEV AND ENGRG CMND
ARMAMENT RSRCH DEV AND ENGRG CNTR
ARMAMENT ENGRG AND TECHNLTY CTR
ATTN AMSRD-AAR-AEF-T J MATTS
BLDG 305
ABERDEEN PROVING GROUND MD 21005-5001

US ARMY TRADOC
BATTLE LAB INTEGRATION & TECHL DIRCTRT
ATTN ATCD-B
10 WHISTLER LANE
FT MONROE VA 23651-5850

PM TIMS, PROFILER (MMS-P) AN/TMQ-52
ATTN B GRIFFIES
BUILDING 563
FT MONMOUTH NJ 07703

SMC/GPA
2420 VELA WAY STE 1866
EL SEGUNDO CA 90245-4659

COMMANDING GENERAL
US ARMY AVN & MIS CMND
ATTN AMSAM-RD W C MCCORKLE
REDSTONE ARSENAL AL 35898-5000

US ARMY INFO SYS ENGRG CMND
ATTN AMSEL-IE-TD F JENIA
FT HUACHUCA AZ 85613-5300

US ARMY SIMULATION TRAIN & INSTRMNTN CMND
ATTN AMSTI-CG M MACEDONIA
12350 RESEARCH PARKWAY
ORLANDO FL 32826-3726

US GOVERNMENT PRINT OFF
DEPOSITORY RECEIVING SECTION
ATTN MAIL STOP IDAD J TATE
732 NORTH CAPITOL ST., NW
WASHINGTON DC 20402

US ARMY RSRCH LAB
ATTN AMSRD-ARL-CI-OK-TP TECHL LIB
T LANDFRIED (2 COPIES)
BLDG 4600
ABERDEEN PROVING GROUND MD 21005-5066

DIRECTOR
US ARMY RSRCH LAB
ATTN AMSRD-ARL-RO-EV W D BACH
PO BOX 12211
RESEARCH TRIANGLE PARK NC 27709

US ARMY RSRCH LAB
ATTN AMSRD-ARL-D J M MILLER
ATTN AMSRD-ARL-CI-OK-T
TECHL PUB (2 COPIES)
ATTN AMSRD-ARL-CI-OK-TL
TECHL LIB (2 COPIES)
ATTN AMSRD-ARL-SE-DE M LITZ
ATTN AMSRD-ARL-SE-DE Y NGU
ATTN AMSRD-ARL-SE-DP B GEIL
ATTN IMNE-ALC-IMS
MAIL & RECORDS MGMT
ADELPHI MD 20783-1197

INTENTIONALLY LEFT BLANK